Available online at www.sciencedirect.com
SCIENCE DIRECT®
Catalysis Today 89 (2004) 83–88
CATALYSIS TODAY
www.elsevier.com/locate/cattod

# Oxidation of propene and the formation of methyl nitrate in non-thermal plasma discharges

Igor Orlandini, Uwe Riedel*

*Interdisziplinäres Zentrum für Wissenschaftliches Rechnen, Universität Heidelberg, Im Neuenheimer Feld 368, D-69120 Heidelberg, Germany*

**Abstract**

Dielectric barrier discharges are being used for plasma remediation of $NO_x$ from the exhaust of internal combustion engines, especially for diesel engines. It was found that unburned hydrocarbons (UHC) present in exhausts play a significant role in altering NO remediation pathways. For a better understanding and optimization of possible applications of this technique, it is necessary to develop models for the underlying physical and chemical processes which are responsible for the removal of pollutants.

The effect of propene and propane on the removal of NO is investigated in this study including the formation of methyl nitrate. In experiments, it has been found that methyl nitrate is an important by-product of the plasma treatment of exhausts.

A volume-averaged model is presented, that can describe the oxidation of hydrocarbons and conversion of NO by a multi-pulse treatment of the exhaust gases at low temperatures and at atmospheric pressure in dielectric barrier discharges. A detailed reaction mechanism is used that takes into account the production of active radicals in every discharge and the reactions induced by these radicals.

Reaction flow analysis and sensitivity analysis are performed to identify specific reaction paths and rate limiting reactions for typical operating conditions of dielectric barrier discharges. A comparison of the oxidation of propene compared to propane, the analogous alkane, is presented.


*Keywords:* Plasma processing; Unburned hydrocarbons; $NO_x$; Diesel engines

## 1. Introduction

Increasingly stringent air quality standards [1] will require future diesel engines to be equipped with exhaust aftertreatment systems to decrease unburned hydrocarbon (UHC) and nitric oxide emissions. The catalytic converters used today in spark-ignited gasoline automobiles are responsible for major reductions in tailpipe emissions of carbon monoxide, hydrocarbons, and $NO_x$. However, these catalysts do not work well on diesel engines, which operate on lean fuel/air mixtures. The exhaust gas from these engines contains an excessive amount of oxygen that inhibits the chemical reduction of $NO_x$ to molecular nitrogen rendering catalytic converters useless for $NO_x$ removal.

$NO_x$ is responsible for acid rain and tropospheric ozone formation. Cold start emissions of unburned hydrocarbons are a dominant fraction of the total hydrocarbon emission. In combination with $NO_x$ emissions hydrocarbons are important precursors of summer smog. Therefore, having a good fuel economy, diesel engines still need to be improved with respect to emissions to gain more widespread use. To achieve this goal, among systems proposed for (diesel) $NO_x$ reduction [1] are those based on non-thermal plasma discharges combined with a catalyst. Especially during the cold start phase the non-thermal plasma processing of NO will help to reduce emissions. The advantage over other systems for exhaust gas cleaning currently under investigation is their high efficiency right after engine start. Furthermore, the use of non-thermal plasma systems for aftertreatment of particulates is under intense investigation, see e.g. [2].

During the last few years, simulation of plasma processing has become a valuable tool. The influence of different parameters like UHC concentration, NO concentration, or carrier gas temperature has been examined theoretically and experimentally [3–7]. Systems combining non-thermal plasma processing and catalytic emission reduction are discussed in [8–11].

* Corresponding author.
*E-mail address:* riedel@iwr.uni-heidelberg.de (U. Riedel).

0920-5861/$ – see front matter © 2003 Elsevier B.V. All rights reserved.
doi:10.1016/j.cattod.2003.11.018

In this paper, we investigate the plasma removal of propene and propane and the oxidation of NO in the presence of these two unburned hydrocarbons. Diesel exhausts inevitably contain unburned hydrocarbons (typically 100–1000 ppm) from incomplete combustion of the fuel, excess oxygen (typically 6–10%) and water (typically 5–12%). Although the composition of these UHCs depends on many factors, e.g. air to fuel ratio, compression ratio, or origin of the fuel, it is instructive to investigate the consequences of selected hydrocarbons on plasma remediation as model cases.

In extension to results published recently [12] the formation of methyl nitrate is considered because in recent experiments [13,14], it has been found that methyl nitrate is an important by-product of the plasma treatment of exhausts. A comparison with different experiments is presented: The temporal evolution of the OH concentrations in single pulse discharges measured with laser induced fluorescence are used for a validation of our model. The experiments of Bröer et al. [15–17]—using propene and propane as a model UHC—is used as a reference system for a comparison of UHC and NO oxidation and to investigate the formation of methyl nitrate.

Reaction flow analysis and sensitivity analysis are performed to identify specific reaction paths and rate limiting reactions for typical operating conditions of dielectric barrier discharges. A comparison of the oxidation of propene compared to propane, the analogous alkane, is presented. The formation of methyl nitrate as a by-product of the oxidation of propene is investigated. The results of our numerical simulation show good agreement with experimental results published in the literature.

## 2. Description of the model

The multi-pulse treatment of mixtures in a plasma reactor is described in a volume-averaged approach by solving for the mass fraction of each chemical species in the reactor, including the re-generation of active radicals by the discharge pulses. The schematic in Fig. 1 shows the relation of the simulation modules *radical generation* (Module 1) and *species tracking* (Module 2). This separation is justified because of the different time-scales of the processes considered: The discharge phase is on the order of a few nanoseconds followed by the metastable quenching phase completed after tens of nanoseconds, and the radical utilization phase is of order 10 μs and longer. In Fig. 2 the temporal evolution of a few key-radicals created in the discharge is shown. The gas mixture consists of 72% $N_2$, 18% $O_2$, and 10% $H_2O$. The effective electrical field $E/n$ is 120 Td. It can be clearly seen from this figure that the radical formation is a very fast process and that there is no overlap with the longer time-scales of NO and UHC reactions.

The radical generation module (Module 1) is used to estimate the concentration of the key-radicals produced initially in the discharge. The radicals O, OH, H, N, and electronically excited species $O(^1D)$, $N(^2D)$, $N(^2P)$, $O_2(a^1\Delta_g)$, and $N_2(A^3\Sigma_u^+)$ are considered. Although a small portion of the carrier gas is consumed by radical production, its

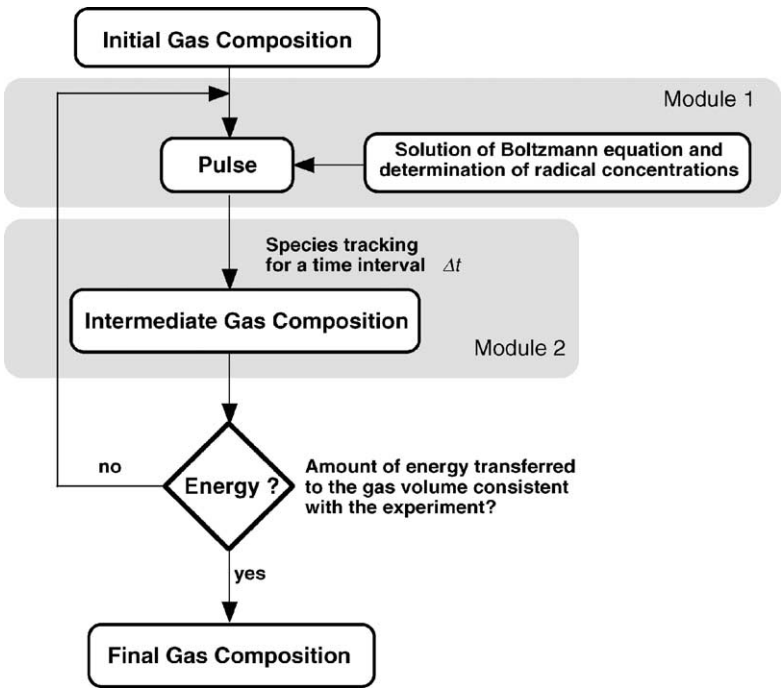


Fig. 1. Schematic of the model: radical generation (Module 1) and species tracking (Module 2).

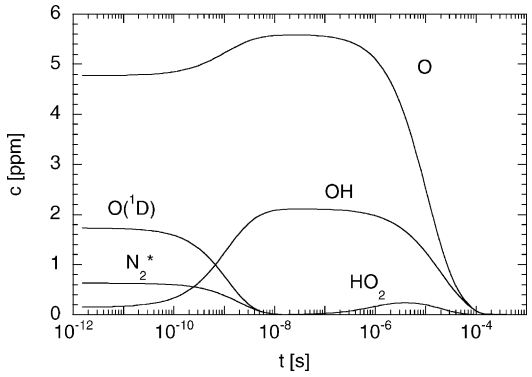


Fig. 2. Temporal evolution of several key-radicals created in a discharge. The effective electrical field $E/n$ is 120 Td. The carrier gas consists of 72% $N_2$, 18% $O_2$, and 10% $H_2O$.

concentration is assumed to be constant. We further assume that the radicals are homogeneously distributed in the discharge streamer, and that changes in temperature are also homogeneous.

The radical concentrations of these species are obtained by multiplying the radical production efficiencies by the energy dissipated for streamer propagation (usually given in J/l). The production efficiency for a given active species (radical or electronically excited molecule) is derived in [4,18]. Details on the implementation can be found in [12].

The rate coefficients for electron-impact reactions strongly depend on the mean electron energy in the discharge plasma. An offline table of electron-impact rate coefficients as a function of the effective electrical field $E/n$ is initially generated by solving Boltzmann's equation for the electron energy distribution function using a two-term spherical harmonic expansion over the $E/n$ range of interest. The solution is obtained using the package `Elendif` [19]. Input to the code are the gas composition, $E/n$, and electron–molecule collision cross sections.

The mean electron energy in most electrical discharge reactors operating at atmospheric pressure is typically 3–6 eV [6]. In this range, a large fraction of the input power goes into formation of O- and $O(^1D)$-radicals although $N_2$ is the major component of the carrier gas (see [12] for details). The dissociation energy of $N_2$ is much higher than that of $O_2$ (9.2 eV compared to 4.8 eV), and consequently, very high mean electron energies are required to produce significant concentrations of N-radicals.

The species tracking module (Module 2) consists of the well-stirred reactor code `Homrun` [20]. The system of conservation equations is solved using an implicit extrapolation method `Limex` [21]. As a result we obtain the evolution of each species between two discharge pulses. After a time interval $\delta t = \nu^{-1}$ depending on the discharge frequency $\nu$ the concentration of the key-radicals is restored to the values obtained in the radical generation module (Module 1) and the time integration continues (see Fig. 1) until the energy transferred to the gas is consistent with the experiment.

## 3. Overview of the reaction mechanism

The detailed reaction mechanism used in this work is built in a hierarchical manner. The core of the mechanism represent the $H_2/O_2$-mechanism and $C_4$-mechanism which was extended by specific reactions important for plasma conditions. It consists of the three main parts: the hydrocarbon mechanism based on the work of Baulch et al. [22], a reaction mechanism, describing the formation and destruction of $NO_x$, and reactions involving electronically excited species [12]. We adopted the Arrhenius parameters for the low temperature range according to literature values and added new reaction paths and new chemical species which are important at given conditions (temperature of the exhaust gas). The rate coefficients used in this work are compiled from different sources and are applicable over the temperature and pressure range encompassed by the experiments.

Essential new chemical species are different partially oxidated hydrocarbons and electronically excited species: $O(^1D)$, $O_2(a^1\Delta_g)$, $N(^2D)$, $N(^2P)$ and $N_2(A^3\Sigma_u^+)$. These species have a direct influence on both the evolution of certain radicals and the NO- and HC-transformation. The most important reactions that enhance NO- and HC-removal involving metastable species are [23]:

$$N(^2D) + O_2 \rightarrow NO + O$$

$$O(^1D) + H_2O \rightarrow OH + OH$$

$$N_2(A^3\Sigma_u^+) + H_2O \rightarrow N_2 + OH + H$$

## 4. Validation

Besides simulations presented already in [5,12] experiments reported recently [24] are used for a further validation of our model. In the experiment, the laser induced fluorescence (LIF)-signal is recorded as a function of time. The initial increase of OH is due to reactions of metastable species with background molecules leading to the formation of additional OH. The LIF measurements record only relative concentrations and therefore the computed peak values have been scaled to match the experiment. The results of our simulations are presented in Figs. 3 and 4. The flow was seeded with different concentrations of either NO or $C_2H_4$.

Fig. 3 shows the temporal evolution of OH radicals for different initial concentrations of NO in the mixture. The carrier gas consist of 92% $N_2$, 8% $H_2O$. The temperature is 373 K and the pressure is 1 bar. The squares represent the experimental values and lines represent the result of the simulation. In this system, OH radicals are consumed in the reaction:

$$NO + OH + M \rightarrow HNO_2 + M$$

Fig. 4 shows the temporal evolution of OH radicals for different initial concentrations of $C_2H_4$ in the mixture. Again,

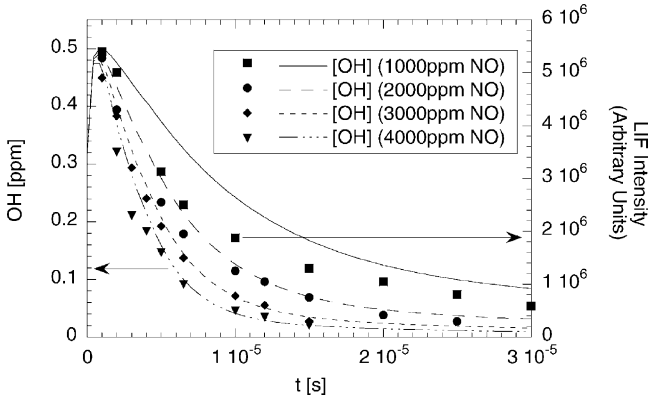


Fig. 3. Temporal evolution of the OH radicals if the flow is seeded with NO. Carrier gas: 92% $N_2$, 8% $H_2O$. Points: experiments [24]; lines: simulations; $T = 373\,K$; $p = 1\,bar$.

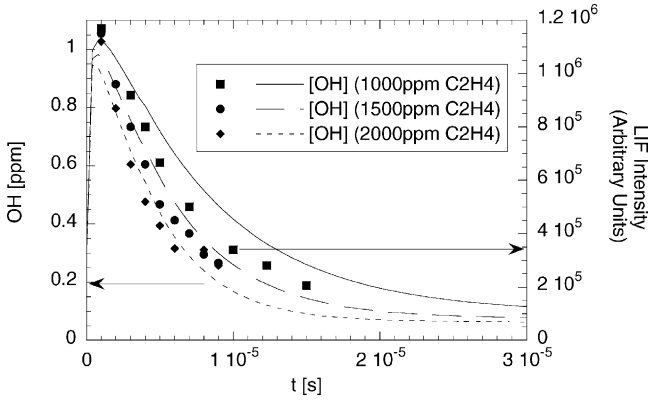


Fig. 4. Temporal evolution of the OH radicals if the flow is seeded with $C_2H_4$. Carrier gas: 88.5% $N_2$, 4.3% $O_2$, 7.2% $H_2O$. Points: experiments [24]; lines: simulations; $T = 373\,K$; $p = 1\,bar$.

the squares represent the experimental values and lines represent the simulation. Here, the carrier gas consists of 88.5% $N_2$, 4.3% $O_2$, 7.2% $H_2O$. The temperature is 373 K and the pressure is 1 bar. In this system, OH radicals are consumed in the OH-addition reaction:

$$C_2H_4 + OH \rightarrow CH_2CH_2OH$$

It can be seen from Figs. 3 and 4 that the change in the OH concentrations is well predicted by our model for concentrations of NO in the range of 2000–4000 ppm and $C_2H_4$ in the range 1500–2000 ppm. For smaller concentrations (1000 ppm) of the two species NO and $C_2H_4$ there is a slight overprediction of the OH-signal in the simulation.

## 5. Oxidation of propene and the formation of methyl nitrate

The effect of propene on the conversion of NO by plasma processing in humid air was examined experimentally by Bröer [15–17] concluding that approximately 30% of the initial $NO_x$ has been reduced to $N_2$ at input energy density of 120 J/l when unburned propene is in the gas mixture. But this finding cannot be verified in simulations and is also in contradiction with the experimental results of Pitz et al. [7].

Our numerical simulations indicate that:

1. The predominant NO reactions are the oxidation to $NO_2$.
2. $HNO_2$ and $HNO_3$ are important by-products of the plasma processing.
3. Methyl nitrates and methyl nitrites are acting as an intermediate storage of nitric oxides enhancing the decrease of $NO_x$ concentrations.
4. Significant differences exist between propene and propane with respect to NO conversion and the consumption of the unburned hydrocarbon itself as a function of the energy transferred to the gas.

These findings will be elaborated in the remainder of this section.

Fig. 5 shows the conversion of NO in $NO_2$ and the by-products $HNO_2$ and $HNO_3$. Plotted are the concentrations versus energy input for a carrier gas containing 500 ppm NO and 500 ppm propene at 473 K. The results of the simulation are plotted as lines and the points represent the experiment. The carrier gas consists of 72% $N_2$, 18% $O_2$, and 10% $H_2O$. Our model reproduces the experimental observations at 473 K well, simulations for a temperature of 373 K show a slight overprediction of the $NO_2$ concentration with the same principal evolution of species concentrations. The effective reduction to $N_2$ is found to be marginal under these conditions. Furthermore, in our simulations we find that $HNO_2$ and $HNO_3$ are important by-products at the reactor outlet.

To address the role of methyl nitrate in plasma exhaust treatment the reaction scheme used in a recent studies [5,12] were extended by implementing additional reaction paths. In a recent experiment [13], substantial amounts of methyl

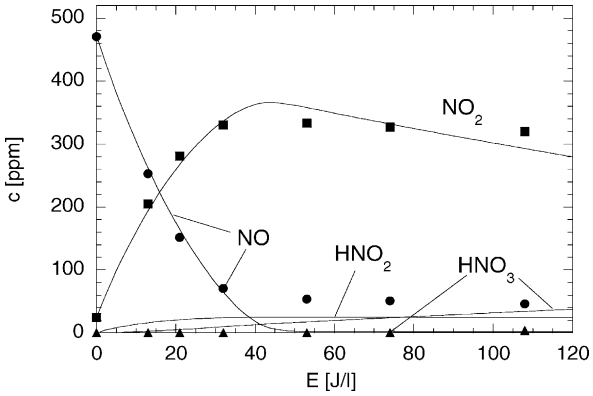


Fig. 5. Conversion of NO at atmospheric pressure in a plasma reactor as a function of transferred energy at $T = 473\,K$. Points: experiments [15,16]; lines: simulations. Carrier gas: 72% $N_2$, 18% $O_2$, 10% $H_2O$. 500 ppm NO, 500 ppm unburned $C_3H_6$. An effective electrical field $E/n$ of 120 Td is used for determination of radical production efficiency.

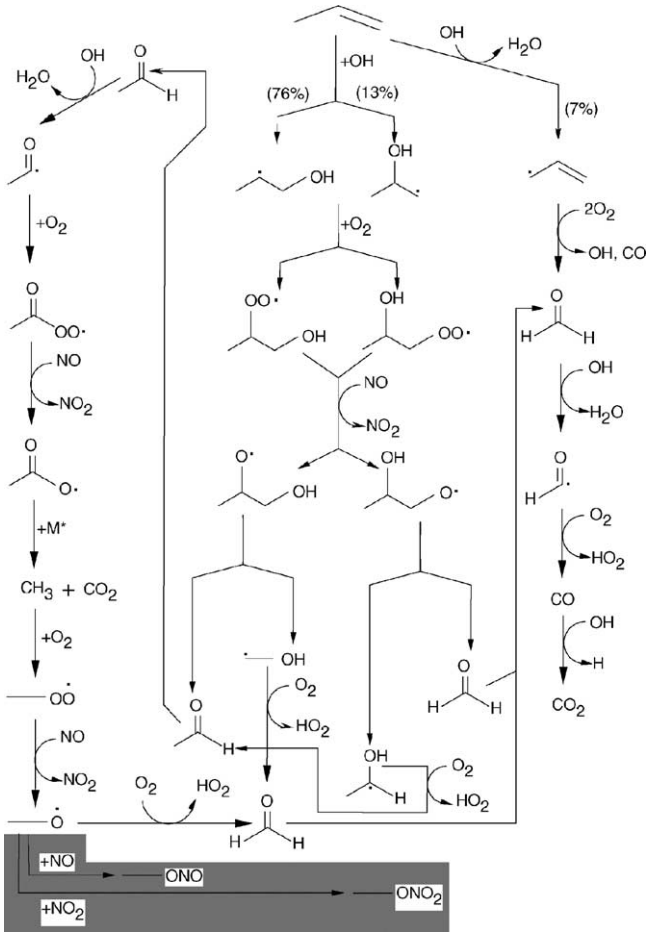


Fig. 6. Dominant reaction pathways for plasma removal of $C_3H_6$. Reaction channels leading to the formation of methyl nitrate are highlighted in gray. See caption of Fig. 5 for conditions.

nitrate have been found. Miessner et al. [14] experimentally investigated mixtures containing 1000 ppm $C_3H_6$ and 500 ppm NO in a carrier gas consisting of 87% $N_2$ and 13% $O_2$. Their results, too, identify methyl nitrate as important by-product of the plasma treatment.

In the simulation, we find that the formation of methyl nitrite is important only in the initial stage of the process due to the rapid conversion of NO into $NO_2$. Methoxy radicals needed to form methyl nitrate in the reaction:

$$CH_3O + NO_2 \rightarrow CH_3ONO_2$$

are provided by the oxidation of acetaldehyde as described in Fig. 6. A further finding in this experiment is that the concentrations of $CO_2$ and $CH_3ONO_2$ show nearly the same evolution of concentrations in the whole range of input energies as long as there is still NO left in the gas mixture. This behavior can be reproduced in the numerical simulation using the mechanism of acetaldehyde oxidation proposed in Fig. 6. NO is consumed at an energy input of 40 J/l (see below, Fig. 8). Up to that energy input $CO_2$ and $CH_3ONO_2$ have a parallel increase in concentration.

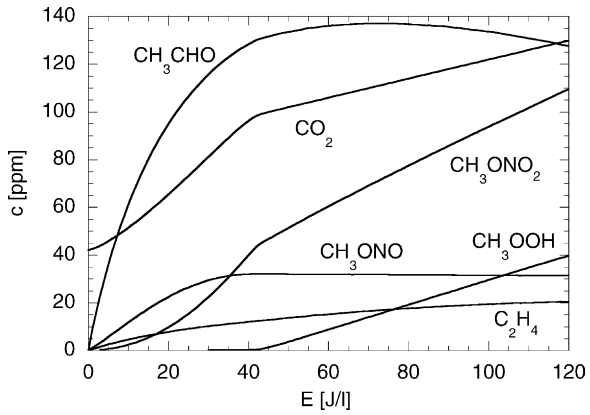


Fig. 7. Formation of methyl nitrate, methyl nitrite and other key species in the plasma processing of a mixture containing 500 ppm $C_3H_6$ and 500 ppm NO. Carrier gas: 72% $N_2$, 18% $O_2$, 10% $H_2O$. An effective electrical field $E/n$ of 120 Td is used for determination of radical production efficiency.

The main reaction paths of $C_3H_6$ oxidation identified in reaction flow analysis and sensitivity studies are summarized in Fig. 6. The sub-mechanism leading to the formation of methyl nitrate (see above) is highlighted in gray. The results of a numerical simulation comparing the plasma oxidation of $C_3H_6$ and $C_3H_8$ is depicted in Fig. 7. The initial concentration of unburned hydrocarbons in the two mixtures compared are 500 ppm $C_3H_6$ (Mixture 1) and 540 ppm $C_3H_8$ (Mixture 2). The carrier gas contains 500 ppm NO, 72% $N_2$, 18% $O_2$, and 10% $H_2O$. Already at 40 J/l energy input transferred from the plasma reactor to the gas volume there is no NO present in the propene mixture, compared to the systems with propane where 80 J/l are needed. Propene itself is consumed much faster than propane (Fig. 8).

The lower reactivity with respect to the gas containing propene can be addressed to the high temperature dependence of H-abstraction reactions:

$$C_3H_8 + \{O, OH\} \rightarrow (i-, n-)C_3H_7 + \{OH, H_2O\}$$

which are needed for the activation of $C_3H_8$ molecules. Contrary to that, oxidation of unsaturated hydrocarbons under

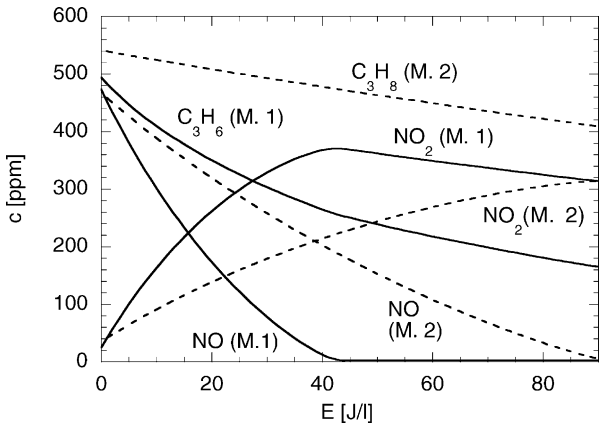


Fig. 8. Comparison of hydrocarbon consumption and NO conversion for propane and propene. (lines: $C_3H_6$, dashed lines: $C_3H_8$).

given low temperature conditions is proceeding through the addition of OH radicals on the π-bond. The activation energy for this reaction is approximately zero [25] and thus the reaction is fast enough at low temperatures. Almost 75% of the initial propane can still be found for an energy input of 80 J/l. Propene is reduced to 40% of its initial concentration already for this energy input.

## 6. Summary and conclusions

This study uses a detailed reaction scheme to access the hydrocarbon and $NO_x$ kinetics in dielectric barrier discharges. Based on estimations for the radical production in each pulse of the discharge, a rate equation model is used to predict concentration changes as the function of time over multiple discharge pulses.

Results for two gas mixtures, $C_3H_6$ and NO in humid air as well as $C_3H_8$ and NO in humid air are reported. We find that in both cases the main path of removal of the initial NO is oxidation to $NO_2$ and later to $HNO_3$ with methyl nitrate being an important by-product acting as a storage of N-atoms. We also find that the mechanism of NO removal is significantly different in the two mixtures examined. The results of our numerical simulations show good agreement with experimental data published in the literature with respect to the concentration variations in time. However, these main processes do not result in an effective net-reduction of $NO_x$.

Therefore, the overall benefit of non-thermal plasma sources is the preconditioning of the exhausts with respect to $NO_x$ and hydrocarbon-compounds creating a chemical composition at the reactor outlet which is favorable for the subsequent treatment in trap-catalysts.

Modeling and numerical simulations describing the composition of the exhausts resulting from the plasma treatment can provide useful information for the design of combined plasma-catalyst systems needed to operate future i.c.-engines with less emissions.

## Acknowledgements

Part of this work was supported by ‘Bundesministerium für Bildung, Wissenschaft, Forschung und Technologie’ under grant 13N7198/5. The authors thank Prof. J. Warnatz, University of Heidelberg, for continuous support and many helpful discussions on reaction kinetics.

## References

[1] C.T. Bowman, Proc. Comb. Inst. 24 (1992) 859.
[2] S.E. Thomas, A.R. Martin, J.C. Whitehead, Non-thermal plasma aftertreatment of particulates, Theoretical limits and impact on reactor design, SAE Technical Papers, No. 2000-01-1926, 2000.
[3] F. Fresnet, B. Baravian, C. Postel, et al., J. Phys. D 33 (2000) 1315.
[4] Y.S. Mok, S.W. Ham, I. Nam, IEEE Trans. Plasma Sci. 26 (1998) 1566.
[5] I. Orlandini, U. Riedel, J. Phys. D 33 (2000) 2467.
[6] B.M. Penetrante, J.N. Bardsley, M.C. Hsiao, Jpn. J. Appl. Phys. 36 (1997) 5007.
[7] W.J. Pitz, B.M. Penetrante, M.C. Hsiao, G.E. Vogtlin, Simultaneous oxidation of NO and hydrocarbons in a non-thermal plasma, in: Proceedings of the Fall Meeting of the Western States Section of the Combustion Institute, 1997.
[8] C. Westbrook, Sci. Technol. Rev. 12 (1999) 4.
[9] H.H. Kim, K. Takashima, S. Katsura, A. Mizuno, J. Phys. D 34 (2001) 604.
[10] M.L. Balmer, R. Tonkyn, S. Yoon, $NO_x$ destruction behavior of select materials when combined with a non-thermal plasma, SAE Technical Papers 1999-01-3640, 1999.
[11] K.P. Francke, H. Miessner, R. Rudolph, Catal. Today 59 (2000) 411.
[12] I. Orlandini, U. Riedel, Combust. Theory Model. 5 (2001) 447.
[13] J.W. Hoard, T.J. Wallington, M.D. Hurley, K. Wodzisz, Environ. Sci. Technol. 33 (1999) 3427.
[14] H. Miessner, K.R. Francke, R. Rudolph, Plasma-enhanced HC-SCR of $NO_x$ in the presence of excess oxygen, Appl. Catal. B: Environmental 943 (2001) 1–10.
[15] S. Bröer, T. Hammer, T. Kishimoto, Proceedings of the 12th International Conference on Gas Discharges and their Applications, vol. 1, Greifswald, 1997, p. 188.
[16] S. Bröer, Plasmainduzierte Entstickung dieselmotorischer Abgase-Der Einfluss gasförmiger Additive sowie die Kombination mit katalytischen und reaktiven Materialien, Ph.D. Thesis, München Technical University, 1998.
[17] S. Bröer, T. Hammer, SAE Technical Papers Series No. 982428, 1998.
[18] L.A. Rosocha, G.K. Anderson, L.A. Bechtold, H.G. Heck, M. Kang, W.H. McCulla, R.A. Tennant, P.J. Wantuck, Treatment of hazardous organic wastes using silent discharge plasmas, in: B.M. Penetrante, S.E. Schultheis (Eds.), Non-thermal Plasma Techniques for Pollution Control, Springer-Verlag, Heidelberg, 1993, p. 282.
[19] W.L. Morgan, B.M. Penetrante, Comput. Phys. Commun. 58 (1990) 127.
[20] U. Maas, J. Warnatz, Combust. Flame 74 (1988) 53.
[21] P. Deuflhard, E. Hairer, J. Zuck, Numer. Math. 51 (1987) 501.
[22] D.L. Baulch, C.J. Cobos, R.A. Cox, G. Hayman, T. Just, J.A. Kerr, T. Murrells, M. Pilling, J. Troe, R.W. Walker, J. Warnatz, P. Frank, Evaluated kinetic data for combustion modelling, J. Phys. Chem. Ref. Data 23 (Supplement I) (1994) 847.
[23] Y. Alekseev, A.V. Levchenko, V.A. Bityurin, Flue gas cleaning by pulse corona, Part II, Technical Report, IVTAN Analytical and Numerical Research Association, Moscow, 1993.
[24] R. Kleinhans, L. Tiase, V. Beushausen, Proceedings of the 27th IEEE International Conference on Plasma Science, New Orleans, LA, 2000.
[25] J. Villa, A. Gonzales-Lafont, J.M. Lluch, J.C. Corchado, J. Espinosa-Garcia, J. Chem. Phys. 107 (1997) 7266.